4-1974

Studies of the Potential Curve Crossing Problem. III. Collisional Spectroscopy of Close Crossings

John B. Delos
William & Mary, jbdelo@wm.edu

Recommended Citation

Delos, John B., Studies of the Potential Curve Crossing Problem. III. Collisional Spectroscopy of Close Crossings (1974). *Physical Review A*, 90(4), 1626-1634.
https://doi.org/10.1103/PhysRevA.9.1626

Studies of the potential-curve-crossing problem. III. Collisional spectroscopy of close crossings

J. B. Delos
Department of Physics, College of William and Mary, Williamsburg, Virginia 23185
(Received 29 October 1973)

Using a previously developed semiclassical theory of electronic excitations, the cross sections that result from potential-curve crossings are calculated for a model system. The phenomena appearing in the differential cross sections are displayed and discussed.

I. INTRODUCTION

In a previous paper,[1] we developed a rather complete theoretical analysis of the two-state potential-curve-crossing problem in atomic collision theory. Our approach was based on a generalization of a method developed by Ovchinnikova and Nikitin[2] and their collaborators for the solution to the coupled "classical-trajectory" equations. In that paper we also showed how such solutions could be combined with elastic scattering phase shifts to obtain the differential cross sections.

At the same time, Olson and Smith[3] and their collaborators were making use of the Landau-Zener theory to analyze the effects that are actually seen in experimental differential cross sections. Such analyses go by the general name of collisional spectroscopy.

The purpose of this paper is to develop the relationship between these two lines of thought. We present here the results of a set of calculations on a "typical" curve-crossing system, making use of the rigorous theory developed in Ref. 1. We focus our attention on the interesting effects that usually occur close to the crossing point (where the Landau-Zener theory is inadequate). The parameters of our typical system were chosen to reflect some similarities to the He^{++}-Ne system and to alkali-halogen-atom systems, which have been the subjects of recent experimental investigations in our laboratory and others.[4] Our results should be useful in the analysis of these and other experiments.

A great deal has already been learned about the nature of such cross sections. For purely repulsive potentials, it is well known that the elastic cross section is smooth at small angles, shows a simple two-term interference pattern at large angles, and at angles close to the crossing threshold, there is a complicated three-term interference pattern. By using the Landau-Zener-Stueckelberg (LZS) approximation, Olson and Smith[3] showed that the small-angle end of this region is marked by a rainbow peak. Also, if the upper state is attractive, Delvigne and Los[5] have shown that the inelastic cross section may show a second peak. The rigorous theory has been applied by Bobbio, Champion, and Doverspike[6] to analyze the collisions of He^+ with Ne. They established the existence of a different rainbow peak, not predicted by LZS theory, marking the large-angle end of the threshold region. This phenomenon was also described somewhat differently by Ovchinnikova and Kotova.[7]

We do not have any spectacular new results to add to the above. However, a complete display of the results of the rigorous theory, and a really clear display of the types of phenomena that appear, have not been presented before. In particular, we wanted to clarify the existence of the two distinct rainbows recognized by Olson[3] and by Bobbio[6]; these have caused confusion in the past, because the one that was first predicted theoretically is not the one that usually appears in the data. In addition, we wanted to see how the phenomena change as the coupling strength is varied. We believe our results provide a rather exhaustive survey of the behavior of differential cross sections for two-state curve crossings, and we hope they will be useful in the analysis of new experimental data.

II. THEORY

In this section we develop the relationships between the solutions to the classical-trajectory equations and the scattering angles and differential cross sections.

We define

$$f_{mn}(\theta) = (2ik_i)^{-1} \sum_L (2L+1) P_L(\cos\theta)(\mathcal{S}^L_{mn} - \delta_{mn}) , \tag{1}$$

where k_i is the magnitude of the wave vector associated with the initial state. The $\underline{\mathcal{S}}$ matrix can be written in two parts,

$$\mathcal{S}_{mn} = e^{i(\eta_m + \eta_n)} S_{mn} \ . \tag{2}$$

The first factor contains only the *elastic* phase shifts for scattering on two potential curves; these can be obtained by quadrature. The second part represents the solution to the classical-trajectory equations [(12) or (17) of Ref. 1]; this factor contains all of the inelastic effects. The inelastic scattering matrix $\underline{S}$ can be factored in the form

$$\underline{S} = \underline{G}\,\underline{\tilde{G}} \ , \tag{3}$$

where $\underline{G}$ (denoted $\underline{G}_+$ in Ref. 1) comes from solving the classical-trajectory equations, making use of their symmetry with respect to time reversal. $\underline{G}$ is a 2×2 unitary matrix, with $\det\underline{G} = 1$, so it can be represented by only three parameters,

$$\underline{G} = \begin{bmatrix} (1-Z^2)^{1/2} e^{i\Gamma_1} & -Ze^{-i\Gamma_2} \\ Ze^{i\Gamma_2} & (1-Z^2)^{1/2} e^{-i\Gamma_1} \end{bmatrix}, \tag{4}$$

where Z represents the transition probability on a single crossing, and Γ_1 and Γ_2 are the associated phases.

These matrices and the phase shifts can be calculated in either the diabatic or adiabatic representations; to within the accuracy of the classical trajectory equations, the full scattering matrix $\underline{\mathcal{S}}$ is invariant to the choice of representation. However, we have found (somewhat to our surprise) that the adiabatic representation is always preferable, because $\underline{G}^A$ is more smoothly varying than $\underline{G}^D$. We will discuss this in detail in Sec. IV; from this point on, however, we assume that all the parameters have been calculated in the *adiabatic* representation.

When the above forms are combined, the resulting scattering amplitudes are as follows: (a) For elastic scattering in the ground state,

$$f_{11}(\theta) = (2ik_1)^{-1} \sum_L (2L+1) P_L(\cos\theta) \times \{(1-Z^2) e^{2i(\eta_1+\Gamma_1)} + Z^2 e^{2i(\eta_1-\Gamma_2)} - 1\} \ ; \tag{5a}$$

(b) for excitation or deexcitation,

$$f_{12}(\theta) = (2ik_1)^{-1} \sum_L (2L+1) P_L(\cos\theta) \times \{2iZ(1-Z^2)^{1/2} e^{i(\eta_1+\eta_2)} \sin(\Gamma_1+\Gamma_2)\} \ , \tag{5b}$$

$$f_{21}(\theta) = (k_1/k_2) f_{12}(\theta) \ ; \tag{5c}$$

(c) for elastic scattering in the excited state,

$$f_{22}(\theta) = (2ik_2)^{-1} \sum_L (2L+1) P_L(\cos\theta) \times \{(1-Z^2) e^{2i(\eta_2-\Gamma_1)} + Z^2 e^{2i(\eta_2+\Gamma_2)} - 1\} \ .$$

Now, in the usual way, we may use the asymptotic approximation for $P_L(\cos\theta)$, and find the points of stationary phase. This leads to deflection functions

$$\Theta_1 = 2\frac{d}{dL}(\eta_1 + \Gamma_1) \ , \tag{6a}$$

$$\Theta_2 = 2\frac{d}{dL}(\eta_1 - \Gamma_2) \ , \tag{6b}$$

$$\Theta_3 = \frac{d}{dL}(\eta_1 + \eta_2 + \Gamma_1 + \Gamma_2) \ , \tag{6c}$$

$$\Theta_4 = \frac{d}{dL}(\eta_1 + \eta_2 - \Gamma_1 - \Gamma_2) \ , \tag{6d}$$

$$\Theta_5 = 2\frac{d}{dL}(\eta_2 + \Gamma_2) \ , \tag{6e}$$

$$\Theta_6 = 2\frac{d}{dL}(\eta_2 - \Gamma_1) \ . \tag{6f}$$

The behavior of these deflection functions and the transition probability provide the means of interpreting the differential cross sections. If the partial-wave summations are carried out by stationary phase, the classical result is obtained, with additional factors representing the interference between the different trajectories. However, the stationary-phase approximation should not be used in the threshold region because of the presence of rainbow extrema in the deflection functions. In Sec. III we present the semiquantal results of the direct numerical summation of Eq. (1).

III. NUMERICAL METHODS AND RESULTS

A. Methods

Calculations have been performed for scattering of 10-eV protons on the pair of potentials of Fig. 1, which are given analytically in the diabatic (crossing) representation by

$$\begin{aligned} V_{11} &= V_{22} + (27.2/R) e^{\eta(1-R/R_{11})} - E_{20} \ , \\ V_{12} &= A_{12} e^{-B_{12}(R-C_{12})^2} \ , \\ V_{22} &= A_{22}\{e^{2C_{22}(1-R/R_{22})} - 2e^{C_{22}(1-R/R_{22})}\} + E_{20} \ , \end{aligned} \tag{7}$$

where (in eV and bohrs)

$$\begin{aligned} &\eta = 6.5, && R_{11} = 4.5, && E_{20} = 5.9, \\ &A_{22} = 0.574, && R_{22} = 3.4, && C_{22} = 2.82, \\ &A_{12} = 2.2, 0.88, 0.29, && B_{12} = 0.444, && C_{12} = 3.0. \end{aligned}$$

The mass used was that of the proton (1836 a.u.) As we mentioned before, these potentials bear a vague similarity to those encountered in collisions of He^{++} with Ne and of alkali metals with halogen

atoms (however, we have cut off the long-range Coulomb potential). Our purpose is not to study any particular system, but to show as clearly as possible the special effects associated with curve crossings. It is noticed that these potentials cross with slopes of opposite sign. As we have emphasized before, such a situation is anomalous if the forces have opposite sign when the crossing point is near the turning point. However, in the present case, when the crossing point and turning point coincide ($L=110$) the centrifugal term $L^2/2MR^2$ makes both effective potentials purely repulsive. Hence, the forces have opposite sign only when L is small, the turning points are far from the crossing point, and the LZS approximation is valid.

In carrying out the partial-wave summations, the range of L can be divided into three regions. For $L \lesssim 80$, $R_{tp} \ll R_x$, and the LZS approximation holds:

$$Z = e^{(-\pi T_0/2)} ,$$

$$\Gamma_1 = -\left[(T_0/2) - (T_0/2)\ln(T_0/2) + \arg\Gamma(iT_0/2) + \pi/4\right] , \tag{8}$$

$$\Gamma_2 = \int_{R_1}^{R_x} k_1(R)\,dR - \int_{R_2}^{R_x} k_2(R)\,dR - \pi ,$$

where all quantities are assumed to be calculated in the adiabatic representation. However, T_0 is related to the diabatic quantities $2V_{12}^2/\hbar v(F_1 - F_2)$.

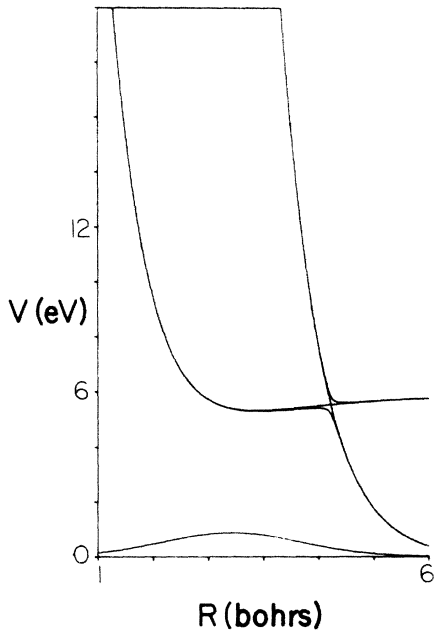

FIG. 1. Potentials V_{11} and V_{22} and coupling V_{12} for $A_{12}=0.88$ (moderate coupling).

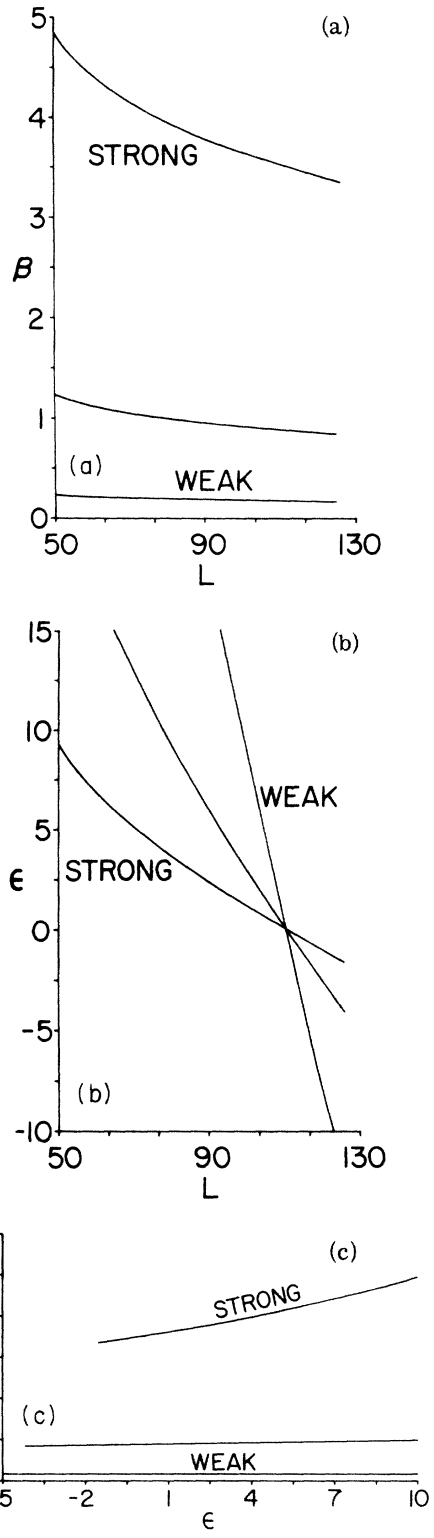

FIG. 2. (a) β vs L for weak, moderate and strong coupling. (b) ϵ vs L for weak, moderate and strong coupling. (c) β vs ϵ for weak, moderate and strong coupling.

To join smoothly to the larger-L region, and to get the interference pattern right, it is essential to use the correct phases as given by Eq. (8).

For $80 \approx L \lesssim 125$, $R_{tp} \sim R_x$, and the LZS approximation cannot be used. Here, $\underline{G}$ must be calculated by direct integration of the classical-trajectory equations. We use the quadratic approximation to $t(s)$ with parameters β, ϵ defined by (see Ref. 1)

$$\beta = \frac{4V_{12}}{\hbar}\left(\frac{MV_{12}}{F(F_1 - F_2)}\right)^{1/2}\left(1 + \frac{2(E - E_x)}{DF}\right)^{-1/2},$$

$$\epsilon = \left(\frac{(E - E_x)(F_1 - F_2)}{2FV}\right)\left(1 + \frac{2(E - E_x)}{DF}\right), \tag{9}$$

$$D^{-1} = \frac{F_1' - F_2'}{F_1 - F_2} - \frac{3V_{12}'}{V_{12}},$$

where all quantities are to be evaluated in the diabatic representation, at the crossing point. The behavior of these parameters is displayed in Fig. 2 for three values of A_{12}. It is seen that ϵ is essentially linearly decreasing with L, and β is essentially constant, except for the case of strongest coupling.

For $L \gtrsim 125$, $R_{tp} \gg R_x$, and the scattering is purely elastic. There are still some interesting effects in the phases Γ_1 and Γ_2 in this region, but Z is so small that they do not appear in the scattering pattern.

We now present three sets of calculations, for V_{12} small, moderate, and large. We analyze the moderate coupling case in great detail, and then the other two.

B. Moderate coupling

In Fig. 3 is a plot of Z^2 as a function of L for all three cases. This is essentially the probability that the system will jump from one adiabatic curve to the other on a single passage through the crossing region. It is seen to have a very steep drop near the threshold region, except in the case of strong coupling. The Landau-Zener (LZ) formula predicts that Z^2 should go to zero at $L_x = 110$, where crossing point and turning point coincide; in fact, Z^2 is non-negligible for some five to ten partial waves into the forbidden region. Except for this, which is not too important, it is rather well predicted by the LZ formula.

We now consider elastic scattering that begins and ends in state 1. In Fig. 4(a) are the 1-1 scattering angles Θ_1 and Θ_2. For large L, small θ, $R_x \ll R_{tp}$, and there is only one path the system can follow (region 1). For small L, there are two paths; Θ_1 is the angle resulting from staying on the lower adiabatic, and Θ_2 is the angle resulting from making transitions to and from the upper adiabatic. As L decreases, and the turning point approaches the crossing point, the repulsive force on the particle abruptly decreases, so the scattering angle stops increasing, and starts decreasing. This turning around results in a stationary point at 4, causing a rainbow peak originally recognized by Bobbio *et al.*[6] For those same values of L, if the system makes a transition up and down, then during the time it spends in the upper state, it feels a much weaker repulsive force. Accordingly, $\Theta_2 < \Theta_1$ in this region (point 3). There are also two stationary points here, but they have no effect on the scattering. As L continues to decrease, Θ_1 continues to decrease for a while, but since it must go to π at $L = 0$, it eventually turns around, resulting in a rainbow first pointed out by Olson.[3] In this range of L, the particles that make transitions feel a strongly repulsive force in the upper state, so $\Theta_2 > \Theta_1$. Clearly, then, Θ_1 and Θ_2 must cross each other at L_x.

The behavior of the scattering angles is clearly manifested in the cross section [Fig. 4(c)]. In region 1, the cross section is smooth (except for some calculation noise). The highest peak at 2 represents the Olson rainbow. Interference between the two branches of this rainbow is represented by oscillations of wavelength about $\pi/10$; this is only recognizable in the envelope (dashed lines). The finer oscillations (wavelength $\pi/40$) result from interference between the pair of branches of the rainbow and the branch of the deflection function that extends into region 1. The

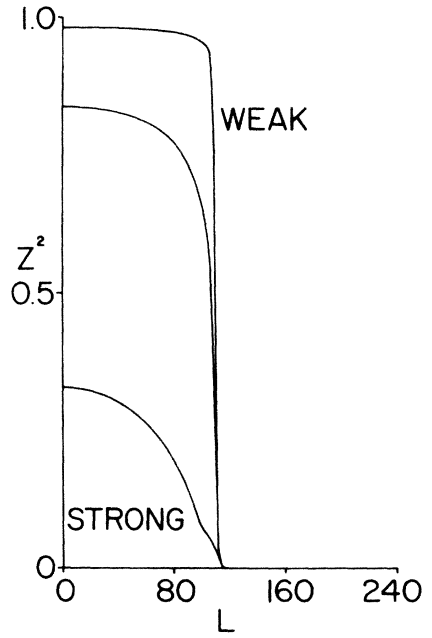

FIG. 3. Z^2 vs L for weak, moderate, and strong coupling.

very large peak at 4 represents the Bobbio rainbow; superimposed on it are fine oscillations due to the interference of its branches with the highest branch of Θ_1. The Bobbio rainbow is generally much more clearly visible than the Olson rainbow (especially on a plot of $\ln\sigma$ vs θ) because both are weighted by the $(1-Z^2)$ factor in the partial-wave sum, and Z^2 is very much larger at small L than at large L. In this case, this factor gives a weight of esentially unity to the Bobbio rainbow, but only 0.2 to the Olson rainbow. In region 6, a simple interference pattern is seen to result from Θ_1 and Θ_2. In principle, it is possible to reconstruct Θ_1 and Θ_2 from this pattern, but this has not yet been done in practice. Finally, we note that the stationary points of region 3 have no influence on the cross section because they are weighted by Z^2 in Eq. (5a).

Let us now go on to consider excitation or deexcitation, starting in state 1 and ending in state 2 or vice versa. The scattering angles are shown in Fig. 5(a). They seem quite similar to Θ_1 and Θ_2 at first glance, but they do have a somewhat different behavior in the threshold region. For large L (region 1), again $R_{tp} \gg R_x$. If the system makes a transition at all, it will do so at the turning point, because it never reaches the crossing point. As a consequence, the deflection function is the average of the deflection functions for elastic scattering on the two potentials. This also can be seen mathematically from Eqs. (6c) and (6d), since both Γ_1 and Γ_2 go to zero in the forbidden region. For small L (region 6) Θ_4 is greater than Θ_3 because the upper curve is more strongly repulsive than the lower curve inside the crossing point. These facts are well known from the LZS theory; however, the behavior of the angles near L_x is not correctly predicted by the LZS approximation. For L just greater than L_x, Θ_3 is greater than Θ_4 because the lower curve is more strongly repulsive than the upper curve outside the crossing point. This results in a set of stationary points near 2 and 3, which, however, have no consequences in the scattering pattern. There is also necessarily a crossover of Θ_3 and Θ_4 at L_x (point 5). It is seen that the angles do not approach L_x with a vertical slope; accordingly, there is no especially dark region there in the differential cross section. Point 4 is the Olson rainbow.

In the 1-2 cross-section curve [Fig. 5(c)], the Olson rainbow is clear, but not spectacular. In contrast to the 1-1 and 2-2 cross sections, there is essentially nothing in the 1-2 cross section that distinguishes the crossing itself, L_x. The stationary points at 2 and 3 are too far into the forbidden region to give maxima in the cross section. The slopes of Θ_3 and Θ_4 at the crossing point, 5, are steep enough to cause a minimum, but the darkening effect of these steep slopes is completely canceled by the behavior of the weighting factor

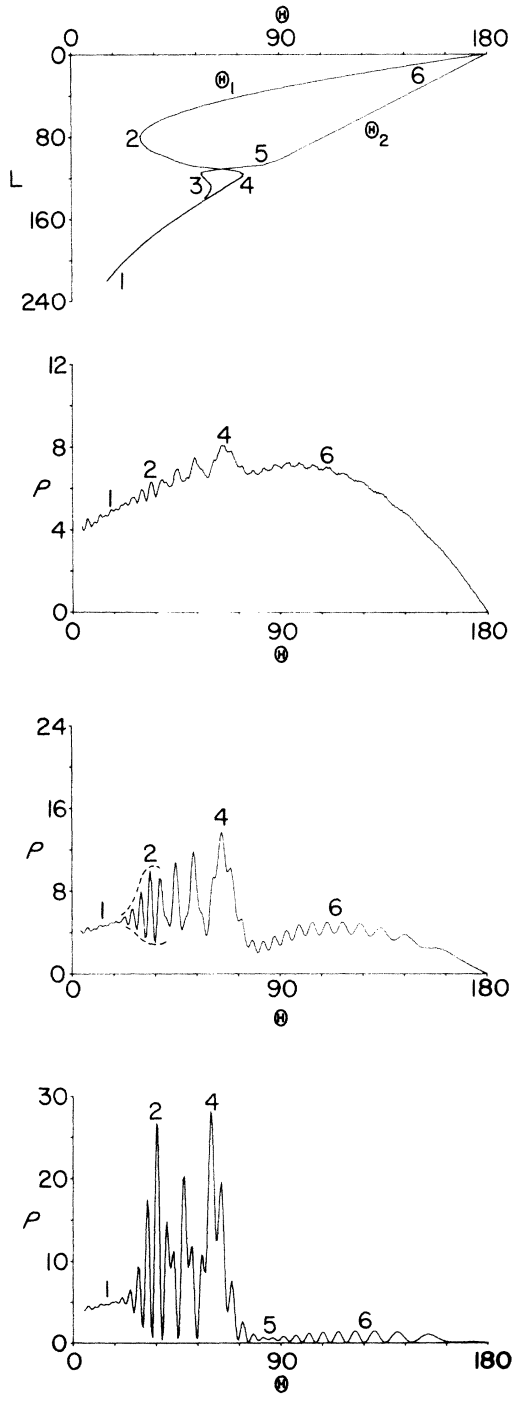

FIG. 4. Elastic scattering in the ground state. 1-1 scattering angles vs L and differential cross sections for weak, moderate, and strong coupling (top to bottom).

$Z(1-Z^2)^{1/2}$, which has a maximum near L_x. On a ρ-vs-τ plot, Θ_x can just be made out at the bottom of a gentle decline in the envelope of the cross section, (5), but it cannot be distinguished in a $\ln\sigma$-vs-θ graph.

Finally, let us consider the elastic scattering that begins and ends in state 2. The scattering angles are shown in Fig. 6(a). In region 1 ($R_{tp} \gg R_x$), they are now negative, because the upper potential is attractive. At point 6, Θ_6, which represents a trajectory entirely on the upper surface, turns around to suddenly become repulsive. This results in a stationary point, 6, and a prominent rainbow that is directly analogous to the Bobbio rainbow in the 1-1 pattern. The behavior of Θ_5 is directly analogous to the behavior of Θ_2 in 1-1 scattering. For $L > L_x$, Θ_5 is more repulsive than Θ_6, while for $L < L_x$, Θ_5 is less repulsive than Θ_6; the same is true of the potentials. As a consequence, there are two stationary points at 2 and 3 in the forbidden region, and a crossover at 4. At point 5 is an ordinary, everyday rainbow that owes its existence to the attractive well in the lower potential.

In the 2-2 cross section, both rainbows are perfectly clear at small angles. The usual one, 5, is slightly lower because it is weighted by Z^2, while the Bobbio rainbow, 6, is weighted by $1 - Z^2$, or essentially unity. The interference pattern here is very complicated, and will never be resolved in practice, because it consists of a superposition of as many as six different terms. At larger angles, 7, the pattern again becomes simple.

C. Weak diabatic coupling (strong adiabatic coupling)

By weak coupling, we mean V_{12} is small; the system usually follows the diabatic curve, so in the adiabatic representation, it is almost certain to make a transition. As a consequence, Z^2 (Fig. 3) is almost a step function. The 1-1 scattering angles (not shown) are essentially the same as those for the moderate coupling case, but it turns out that the crossover near L_x is sharper. In the cross section (Fig. 4), the Bobbio rainbow is clear (4) but the Olson rainbow is scarcely visible (2). Both are weighted by $(1 - Z^2)$, which is essentially unity at $L = 110$, but very small at $L = 80$. In the 1-2 cross section, at small angles, the pattern terminates in the Olson rainbow, which is not a high peak. It is completely impossible to determine Θ_x from the cross section; the behavior of the scattering angles at 4 gives neither peak nor valley in the scattering pattern. In the 2-2 cross section, the usual rainbow, 5, is higher than the Bobbio rainbow, 6, which must slowly disappear

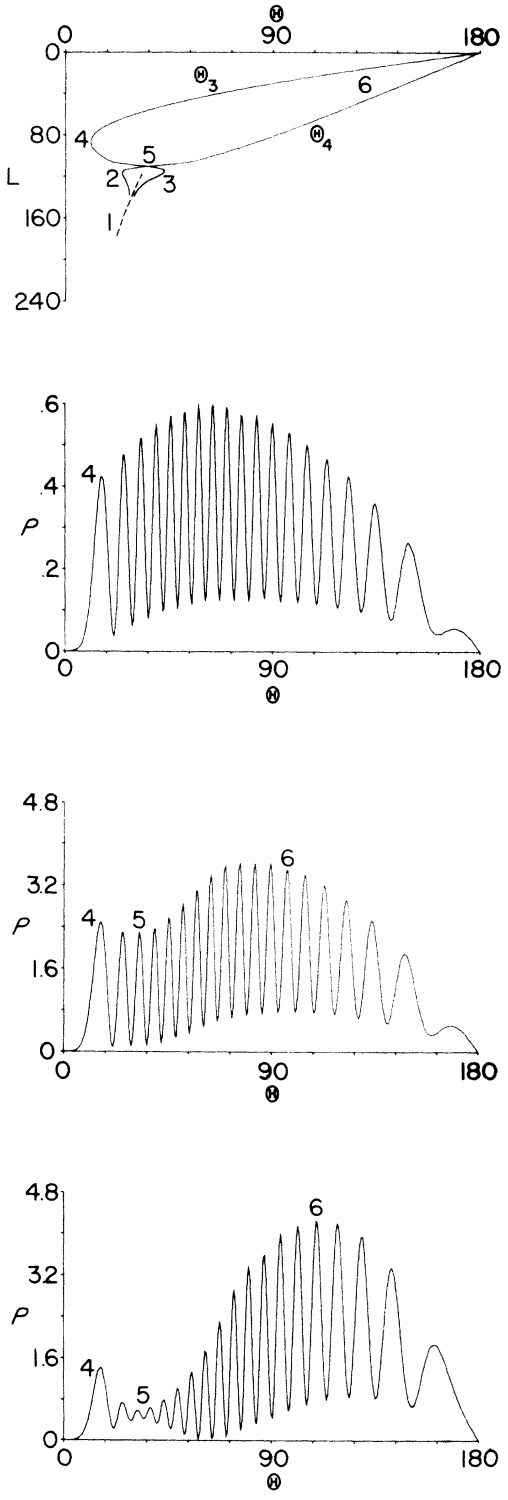

FIG. 5. Excitation from ground state to excited state. 1–2 scattering angles vs L and differential cross sections for weak, moderate, and strong coupling (top to bottom). The numbered points are explained in the text.

in the limit of very weak coupling. In both of the elastic cross sections (1-1 and 2-2) the interference pattern is scarcely visible at large angles, but in the inelastic (1-2) cross section it is equally strong everywhere (but note the scale).

D. Strong diabatic coupling (weak adiabatic coupling)

Strong diabatic coupling means here V_{12} is large; the system tends to remain on the adiabatic (noncrossing) curves, and Z^2 is small. The 1-1 angles (not shown) are essentially the same as before, but more rounded; also, there is a somewhat steeper rise in Θ_2 at 5. In Fig. 4(d) we see that the Bobbio and the Olson rainbows are about equally prominent in the cross section (2, 4). The steep slope of Θ_2 at 5, together with the small value of Z^2, leads to a relatively dark region with little interference just past the Bobbio rainbow [point 5 in Figs 4(a) and 4(d)]. The 1-2 angles are analogous. However, in this case, the Olson rainbow stands out dramatically (4) in the cross section, and we can now see Θ_x marked as a relatively dark region with little interference (5). This is what had been predicted by the LZS formula,[3] and is a manifestation of the greater accuracy of LZS theory for strong coupling. (However, at extremely strong coupling, the LZS theory and the parabolic approximation used here again deviate from the exact result.[8]) In the 2-2 cross section, the usual rainbow (5), weighted by Z^2, is very small, while the Bobbio rainbow, weighted by $(1 - Z^2)$, is quite prominent (6).

IV. ON THE USE OF THE DIABATIC REPRESENTATION

The diabatic or crossing representation is preferred by many who engage in curve-crossing studies, and much effort has been well spent on obtaining formal definitions and properties of such a representation.[9] Our experience has been that derivations and formal work are generally simpler in the diabatic representation, especially for weak coupling, and also in some strong-coupling situations. However, for the kinds of numerical calculations carried out in this paper, the diabatic representation has an important disadvantage: The $\underline{G}$-matrix parameters in the diabatic representation do not behave as simply as the corresponding parameters in the adiabatic representation.

In Fig. 7(a) is shown $(Z^D)^2$ as a function of L for the case of moderate coupling. At large L it goes to zero, of course, and at small L it oscillates about the LZ result $(1-e^{-\pi T_0})$. Similar oscillations in Γ_1 and Γ_2 lead to the scattering angles shown in Fig. 7(b). These angles are qualitatively similar to those obtained from the adiabatic rep-

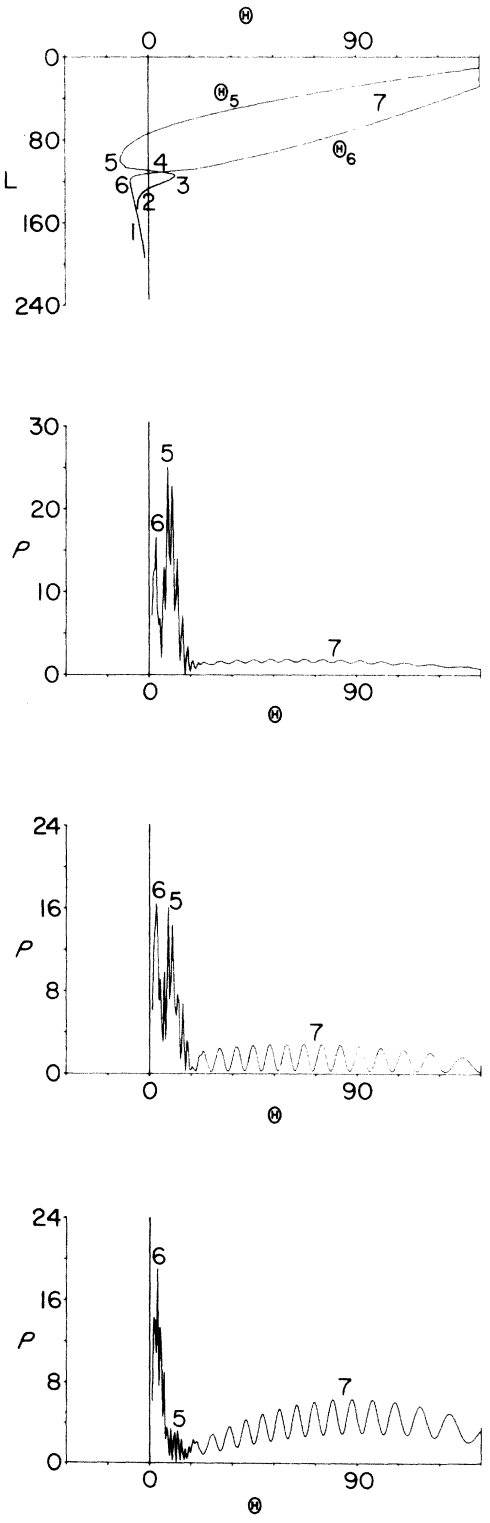

FIG. 6. Elastic scattering in the excited state. 2-2 scattering angles vs L and differential cross sections for weak, moderate, and strong coupling.

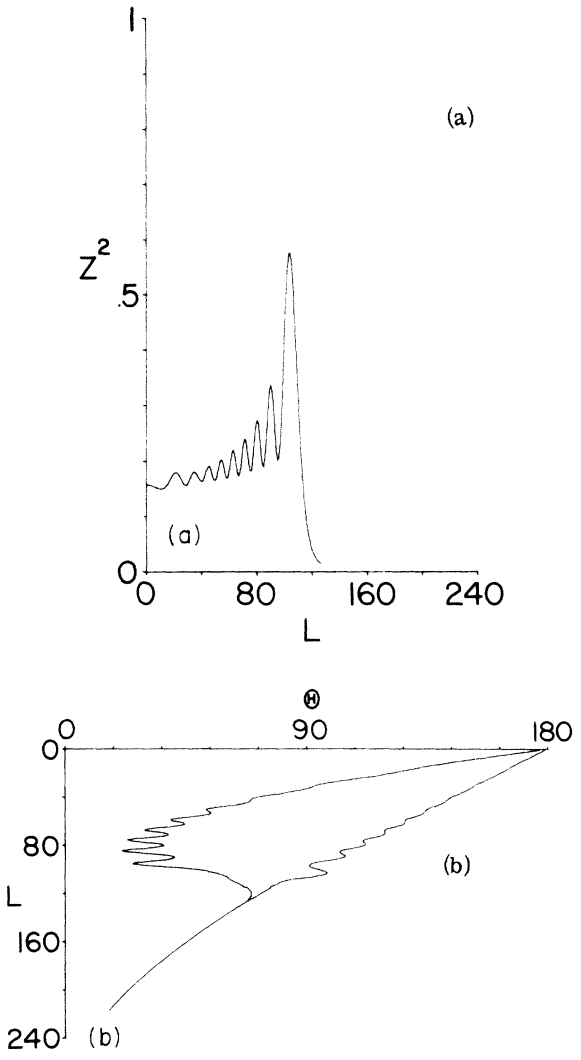

FIG. 7. (a) Z^2 vs L as calculated in the diabatic representation. (b) 1-1 scattering angles vs L as calculated in the diabatic representation.

resentation, but they have small, rapid oscillations which make semiclassical interpretations disquieting, if not completely wrong. These oscillations arise from the exact solutions to the coupled classical-trajectory equations for G_+ [Ref. 1, Eqs. (22) and (28b)], and they are not an artifact of any further approximations. The same oscillations arise whether the phases are calculated directly in the diabatic representation, or transformed to the diabatic representation from adiabatic calculations; they also appear in analytic expressions in the weak coupling limit [Ref. 1, Eq. (53b)].

As we have emphasized before, the $\underline{S}$ matrix and the cross sections are invariant to the representation, provided that the semiclassical approximations are valid. The parameters of the $\underline{S}$ matrix, while complicated, have a direct physical interpretation. But when $\underline{S}$ is factored, as in Eq. (3), there is nothing to guarantee that the resulting parameters will be well behaved, or that they will have a simple physical interpretation. The calculations show that these parameters are well behaved in the adiabatic representation, but not in the diabatic representation.

V. SUMMARY AND CONCLUSIONS

As stated in the introduction, the LZS theory is not too bad for calculating the phenomena resulting from curve crossings. It fails in the threshold region, where the complete theory predicts two additional phenomena. First, there is a second rainbow peak, resulting from a maximum in one of the adiabatic scattering angles. Second, for strong coupling only, there is a dark region with no interference structure close to the threshold region. This could be called an antirainbow, because it results from the very steep slope of the deflection function.

Each of these phenomena has either been identified or at least speculated upon before.[3,6,7] Our only contribution is to present a systematic survey of cross sections in such a way that all of the phenomena can be seen together; thus the significance of each is made clear. Of course, in any given cross section, they will not all appear. For example, if both potentials are attractive, the Bobbio rainbow will not appear in the 1-1 cross section, and if both are repulsive, it will not appear in the 2-2 cross section. Also, in many cases, the two rainbows will not be distinguishable, but will appear superimposed on each other. Nevertheless, it is hoped that this presentation provides a useful guide to "what to look for" in interpreting experiments.

ACKNOWLEDGMENTS

I thank R. L. Champion and L. D. Doverspike for providing the stimulus to carry out these calculations. This research was supported in part by the National Science Foundation, and by NASA under Grant No. NGL-47-006-055.

[1]J. B. Delos and W. R. Thorson, Phys. Rev. A 6, 728 (1972).
[2]V. Bykhovshii, E. E. Nikitin, and M. Ya. Ovchinnikova, Zh. Eksp. Teor. Fiz. 47, 750 (1964) [Sov. Phys.—JETP 20, 500 (1965)]; E. E. Nikitin and M. Ya. Ovchinnikova, Usp. Fiz. Nauk 104, 379 (1971) [Sov. Phys.-Usp. 14, 394 (1972)].
[3]For example, R. E. Olson and F. T. Smith, Phys. Rev. A 3, 1607 (1971), and subsequent papers.
[4]T. L. Bailey (personal communication); C. E. Young (personal communication).
[5]G. A. L. Delvigne and J. Los, Physica 59, 61 (1972).
[6]S. M. Bobbio, R. L. Champion, and L. D. Doverspike, Phys. Rev. A 7, 526 (1973).
[7]L. P. Kotova and M. Ya. Ovchinnikova, Zh. Eksp. Teor. Fiz. 60, 2026 (1971) [Sov. Phys.—JETP 33, 1092 (1971)].
[8]J. S. Cohen, S. A. Evans, and N. F. Lane, Phys. Rev. A 4, 2248 (1971).
[9]M. Barat and W. N. Lichten, Phys. Rev. A 6, 211 (1972); F. T. Smith, Phys. Rev. 179, 111 (1969).